



MINISTRY OF AVIATION

AERONAUTICAL RESEARCH COUNCIL  
REPORTS AND MEMORANDA

A Study of Slender, Cambered, Conical Wings  
by an Electrical Resistance Network

By H. S. WARD, B.Sc.

DEPARTMENT OF CIVIL ENGINEERING,  
UNIVERSITY OF BIRMINGHAM

LONDON: HER MAJESTY'S STATIONERY OFFICE

1964

FIVE SHILLINGS NET

# A Study of Slender, Cambered, Conical Wings by an Electrical Resistance Network

By H. S. WARD, B.Sc.

DEPARTMENT OF CIVIL ENGINEERING,  
UNIVERSITY OF BIRMINGHAM

---

*Reports and Memoranda No. 3369\**

*December, 1962*

---

## *Summary.*

An electrical resistance network for solving the Laplacian field equation has been used to determine the attached-flow incidence of thin slender wings with different forms of camber. This incidence was found by applying the wing boundary condition exactly at the wing's surface.

The lift and induced drag have not been evaluated for the wings studied. Comparison of the stream function obtained from an experiment with that of a known theoretical solution has shown that there should be no difficulty in determining the loading of such wings at the attached-flow incidence.

There appears to be no reason why this method could not be extended to provide a means of analysis of cambered wings with a given thickness distribution.

---

## *1. Introduction.*

Simplifications are often introduced when studying the flow about slender wings at small incidence. Among these is included the assumption that the velocity derivative  $\partial U/\partial x$  is small (Fig. 1). Slender-wing theory then reduces the problem to an analysis of the two-dimensional cross-flow plane. If the restrictions of the theory are met the flow is described by the Laplacian field equation, with the appropriate boundary conditions at a large distance from the wing and those at the wing surface.

The boundary condition applied at a thin solid wing is the elimination of the normal component of the flow's velocity at the wing's surface. If the wing is cambered then this condition is normally applied on some simpler surface near to it. This process may then be called a linearization of the wing boundary condition.

For sharp-edged conical wings there is a particular incidence at which the singularity in the pressure and velocity disappear at the leading edge. It has been shown<sup>1</sup> that the value of this incidence is a function of the location of the wing boundary conditions.

It is at this particular incidence that leading-edge separation can be avoided and the flow parameters calculated from a simple mathematical model. Recent design work<sup>2</sup> has shown that attached flow on slender delta wings is associated with steep gradients of the wing near the leading edge.

---

\* Replaces A.R.C. 24 360.

It therefore became clear that there was a need to assess the reliability of the linearized boundary condition for such configurations.

A general analytic approach to the problem is difficult because of the limited number of conformal transformations which are available. Cooke<sup>3</sup> has carried out some theoretical work for camber distributions of practical interest, at the attached-flow incidence.

Smith<sup>1</sup> has formulated the problem, and because of the difficulty of producing a general analytic solution it appeared that an electrical-analogue approach might prove fruitful.

## 2. Formulation of the Problem.

Consider a wing sufficiently slender to allow the linearized potential equation to be adequate at the Mach design number. The leading edge is sharp and no singularity exists there. Taking a right-handed co-ordinate system, Fig. 1, the undisturbed stream velocity  $U$  is at a small incidence  $\alpha$  to the axis  $Ox$ .

The velocity potential of the flow is given by<sup>4</sup>,

$$\Phi = Uz\alpha + Ux + U\phi, \quad (1)$$

where  $\phi$  is the perturbation potential.

If the problem is restricted to conical wings without thickness the equation of the wing surface becomes,

$$F(x, y, z) = [r - Kxf(\theta)] = 0, \quad (2)$$

where  $K = \cot \lambda$  (Fig. 1).

The boundary condition on the three-dimensional wing surface is,

$$V \times F = 0, \quad (3)$$

this equation represents the vector product of the velocity of flow,  $V$ , and  $F(x, y, z)$ .

If  $K^2 \ll 1$ , the velocity normal to the contour in the cross-flow plane due to the component  $U$ , is given by,

$$\Phi_n \cdot F_n + U \cdot F_x = 0, \quad (4)$$

where

$$\Phi_n = \frac{\partial \Phi}{\partial n}, \quad F_x = \frac{\partial F}{\partial x}, \quad F_n = \frac{\partial F}{\partial n}.$$

Equation (4) is the equivalent two-dimensional expression of equation (3).

Equation (4) may now be written as,

$$\Phi_n = \frac{-UF_x}{F_n} = \pm \frac{UF_x}{(F_y^2 + F_z^2)^{1/2}}. \quad (5)$$

Now consider the conjugate stream function  $\Psi$ .

Then,

$$\frac{\partial \Psi}{\partial \sigma} = -\frac{\partial \Phi}{\partial n} = \frac{UF_x}{F_n}. \quad (6)$$

The value of  $\Psi$  on the cross-section of the wing can be calculated by evaluating the integral,

$$\int_A^B \frac{\partial \Psi}{\partial \sigma} d\sigma = \Psi_B - \Psi_A = U \int_A^B \frac{F_x}{F_n} d\sigma = \frac{2U}{x} \int_A^B \frac{1}{2} r^2 d\theta. \quad (7)$$

If  $\Psi_A$  is arbitrarily made zero then,

$$\Psi_B = \frac{2U}{x} [\text{Area OAB}] \quad (\text{Fig. 1}). \quad (8)$$

The remaining boundary condition to impose on the conjugate function  $\Psi'$  is the correct value at a large distance from the wing. At such points the perturbation potential  $\phi$  is zero and therefore,

$$\Psi'_\infty = -U\alpha y. \quad (9)$$

### 3. Application of the Problem to the Analogue.

The electric resistance network used during this study has been developed by Redshaw<sup>5</sup>. Briefly, it consists of a series of four equal resistors,  $R$ , connected to each node of a network, (Fig. 2). If the current,  $i$ , drawn from the node marked 0 is zero, then

$$\begin{aligned} i = i_1 + i_2 + i_3 + i_4 &= \frac{V_1 - V_0}{R} + \frac{V_2 - V_0}{R} + \frac{V_3 - V_0}{R} + \frac{V_4 - V_0}{R} \\ &= \sum_{n=1}^4 \left( \frac{V_n}{R} \right) - \left( \frac{4V_0}{R} \right) = 0, \end{aligned} \quad (10)$$

where  $V$  is the electrical potential at the nodes, and  $R$  is the value of the resistors connecting the nodes.

If now a function  $\phi$ , which satisfies Laplace's equation, is specified at four points distance  $h$  from the value  $\phi_0$  then the finite-difference form of Laplace's equation is,

$$\sum_{n=1}^4 \left( \frac{\phi_n}{h^2} \right) - \left( \frac{4\phi_0}{h^2} \right) = 0. \quad (11)$$

Equations (10) and (11) show that a square network of equal resistors may be used to represent a Laplacian field. The experimental set up is shown in Fig. 3. The final size of the network was  $144 \times 136$  mesh intervals.

The solution of any given problem involving the Laplace field equation can then be obtained from the analogue when the appropriate boundary conditions have been established.

Equations (8) and (9) provide these conditions. During this study only unyawed wings were considered; this means that the centre-line of the wing cross-section is an axis of symmetry.

The experimental arrangement used during the study may be understood by reference to Fig. 4.

The axis of symmetry representing the centre-line of the unyawed wing was simulated by raising the left-hand edge of the network to a constant potential  $V_L$ .

Equation (9) was satisfied by earthing the right-hand edge of the board and raising it to another constant potential  $V_R$ .

For any given cambered wing it was possible to calculate the value of  $\Psi'$  on the wing from equation (8). The electric potential corresponding to this value of  $\Psi'$  was then easily set up on the electrical network by means of the boundary-condition potentiometers.

The given boundary conditions and the potential distributions were set up and measured by a null-point method. This measuring circuit was made up of a galvanometer and an accurate variable 10 000 ohm resistor as shown in Fig. 4.

The parameter  $\alpha$  in equation (8) can be replaced by the equivalent factor  $S/K$  and this gives,

$$\Psi_B = \frac{2UK}{S} [\text{Area OAB}]. \quad (12)$$

$S$  is the semi-span of the wing and  $K$  the cotangent of the leading-edge sweep angle.

The object of the experimental work was first to determine the incidence, for any given cambered wing, at which the singularity in the pressure and velocity disappeared at the leading edge.

With the analogue layout shown in Fig. 4, this variation of wing incidence was easily simulated. It was achieved by varying the potential at the right-hand edge of the board,  $V_R$ , while  $V_L$  and the potentials on the wing cross-section were kept constant. The incidence was then specified in terms of  $V_L$  and  $V_R$  by equation (9).

$$(V_R + V_L) = U\alpha b, \quad (13)$$

where  $b$  is the number of mesh intervals between the left and right sides of the analogue.

The adjustment of  $V_R$  was controlled by the 10 000 ohm and 200 ohm potentiometers. The 10 000 ohm potentiometer provided a course adjustment, and accurate control was exercised by means of the 200 ohm potentiometer.

The 20 ohm potentiometer was placed in the circuit to reduce the current drainage from the batteries. This was necessary because forty boundary-condition potentiometers were placed in parallel. This meant that there was a low resistance across the 2 volt battery, which would have given a large current flow. This was avoided by the use of the 20 ohm resistance.

#### 4. *Experimental Results.*

To assess the accuracy of the analogue arrangement, a series of experiments was conducted to give a comparison with some known theoretical solutions. The models chosen were of a circular cross-section and the theoretical solutions were due to Smith<sup>1</sup>.

The incidence of the wing was altered until the potential measurements showed that the tangential velocities, on the upper and lower surface, at the leading edge were the same. The incidence of attached flow was determined by plotting the two tangential velocities for different values of the parameter  $\alpha/K$ . The two velocities were found to be directly dependent upon  $\alpha/K$  and the plotted lines crossed at the attached-flow incidence.

A comparison of the experimental and theoretical results for circular wings with different values of  $\beta$  is shown in Fig. 5. The results given in Fig. 6 show the experimental and theoretical values of  $\Psi/KUS$  at the attached-flow incidence for a circular cambered wing with  $\beta = 0.75$ . The lower set of figures, included in the experimental results, are the electrical potentials as read on the network; the figures above represent these numbers converted into terms of  $\Psi/KUS$ . These results confirm the possibility of using the analogue method as a design method in the analysis of thin cambered wings at the attached-flow incidence.

After these preliminary investigations, wings not so amenable to theoretical analysis were studied. Thus Figs. 7 and 8 show the plots of the tangential velocities at the leading edge, of different parabolic wings, against the parameter  $\alpha/K$ . It can be seen from these results that the attached-flow parameter is given by the point where the curves of the inside and outside tangential velocities cross.

The final form of camber considered in this initial study was that of wings with an elliptical cross-section. The results are given in Fig. 9.

Finally the attached-flow parameter  $\alpha/K$  for different values of  $\beta$  for circular, parabolic and elliptical camber is plotted in Fig. 10.

### 5. Conclusions.

The initial study has shown that the electrical-resistance analogue provides a simple method for investigating the attached flow of any form of slender cambered wing, with the exact boundary conditions applied at its surface.

The methods presented here would provide a useful experimental technique for determining the aerodynamic forces acting on such slender wings under the conditions of attached flow.

No serious difficulties should be experienced in extending this work to investigate thick cambered wings.

---

### REFERENCES

<i>No.</i>	<i>Author(s)</i>	<i>Title, etc.</i>
1	J. H. B. Smith .. ..	The properties of a thin conically cambered wing according to the slender-body theory. A.R.C. R. & M. 3135. March, 1958.
2	J. Weber .. ..	Design of warped slender wings with the attachment line along the leading edge. A.R.C. 20,051. September, 1957.
3	J. C. Cooke .. ..	Properties of a two-parameter family of thin conically cambered delta wings by slender-body theory. A.R.C. R. & M. 3349. July, 1960.
4	G. N. Ward .. ..	<i>Linearised theory of steady high-speed flow.</i> Part III. Cambridge University Press. 1955.
5	S. C. Redshaw .. ..	The use of an electrical analogue for the solutions of a variety of torsion problems. <i>Brit. J. App. Phys.</i> , Vol. II, pp. 461 to 468. October, 1960.

---

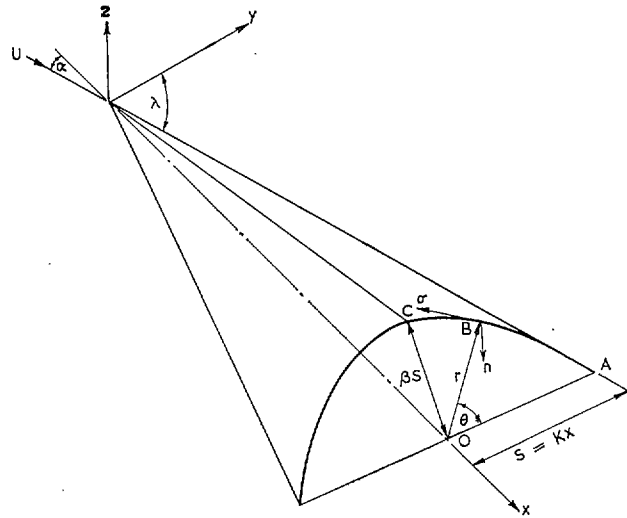


FIG. 1. Co-ordinates of a cambered wing.

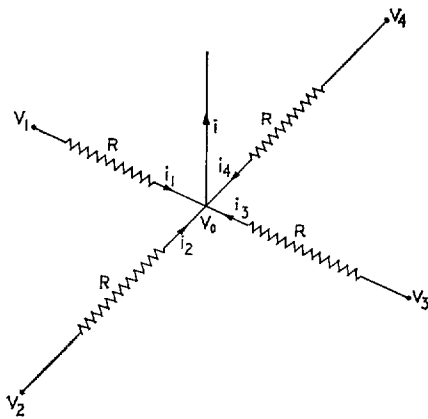


FIG. 2. Network arrangement.

(89339)

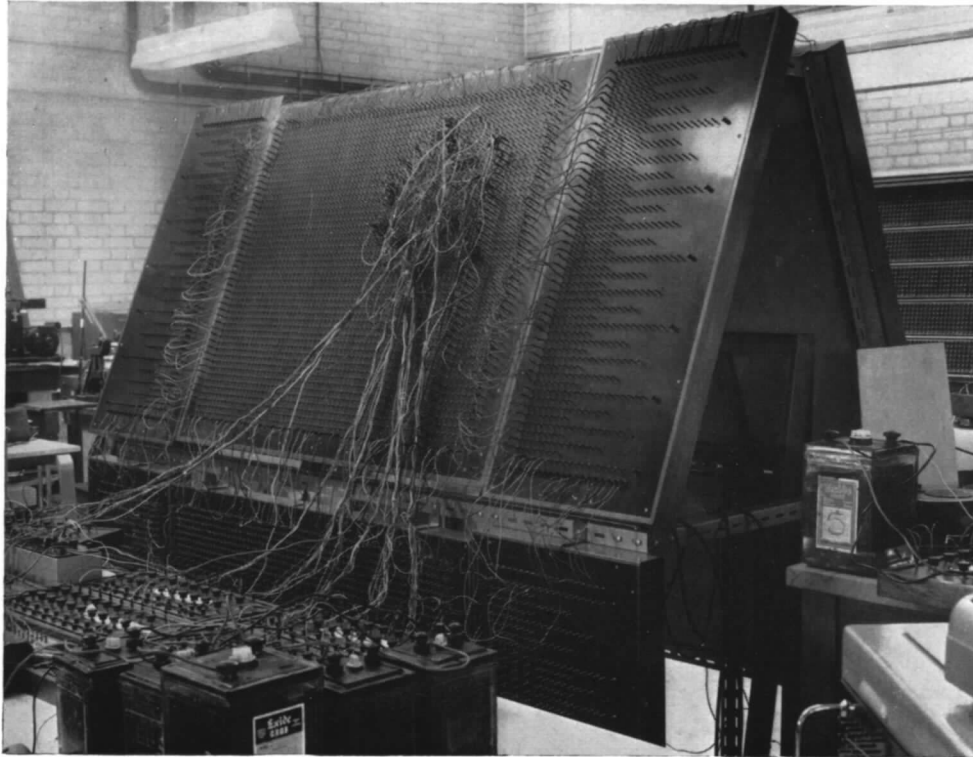


FIG. 3. Construction of the network.

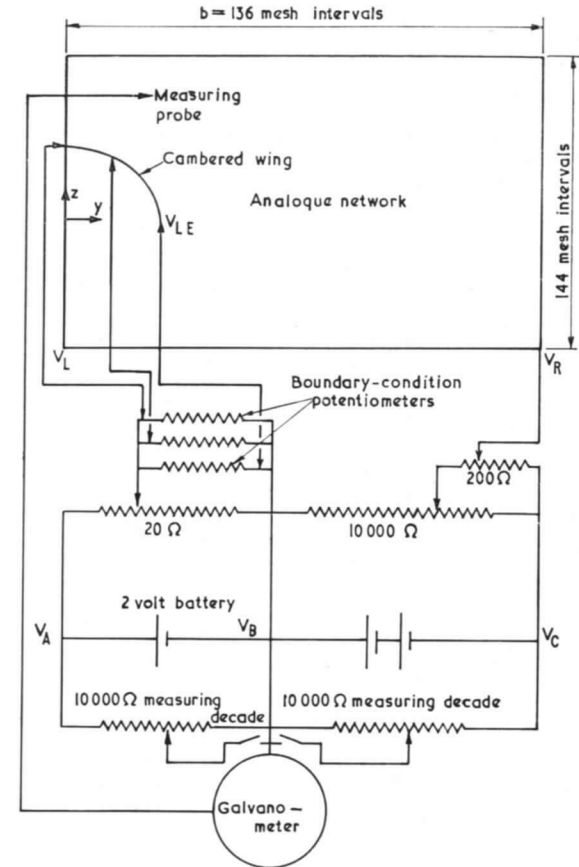


FIG. 4. The cambered-wing circuit.

7

B\*



8

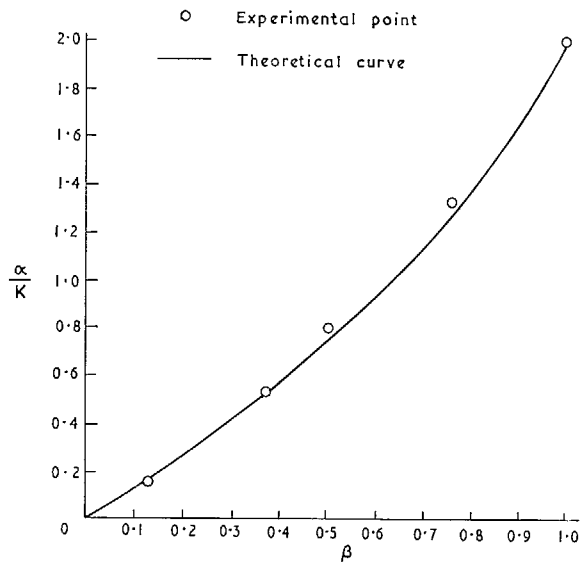


FIG. 5. The attached incidence of circular cambered wings.

z	y	15	16	17
3		-0.940	-1.055	-1.164
2		-0.961	-1.063	-1.171
+1		-0.992	-1.079	-1.184
0		-1.022	-1.105	-1.201
-1		-1.046	-1.130	-1.219

Theoretical

z	y	15	16	17
3		-0.940	-1.060	-1.168
		-0.1657	-0.1867	-0.2059
2		-0.971	-1.070	-1.176
		-0.1712	-0.1885	-0.2073
+1		-1.003	-1.082	-1.189
		-0.1768	-0.1906	-0.2095
0		-1.032	-1.112	-1.207
		-0.1819	-0.1959	-0.2127
-1		-1.054	-1.137	-1.226
		-0.1857	-0.2004	-0.2160

Experimental

FIG. 6.  $\psi/KUS$  for circular camber,  $\beta = 0.75$ .

6

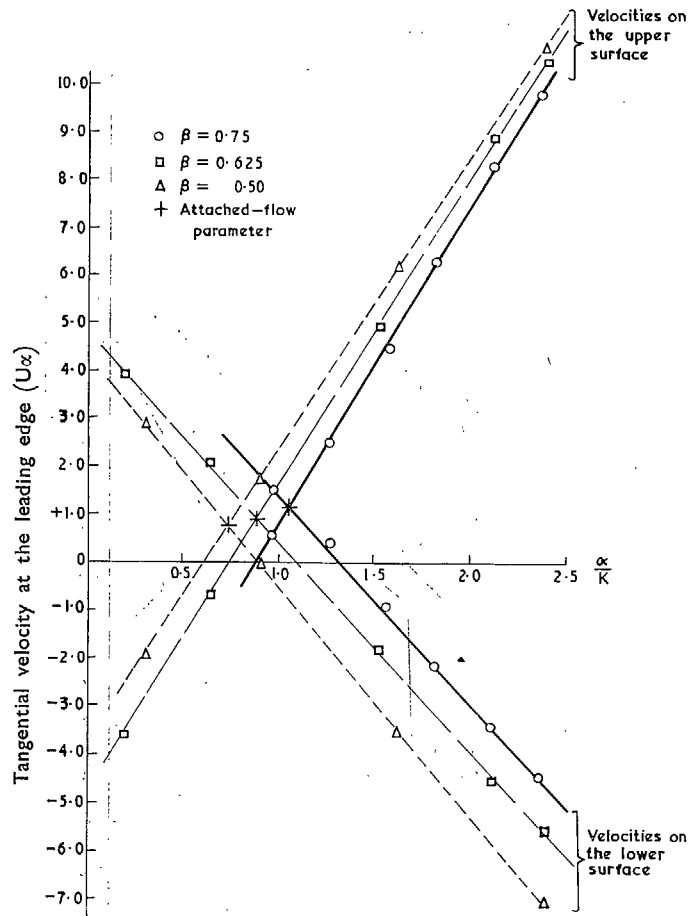


FIG. 7. Parabolic-wing results.

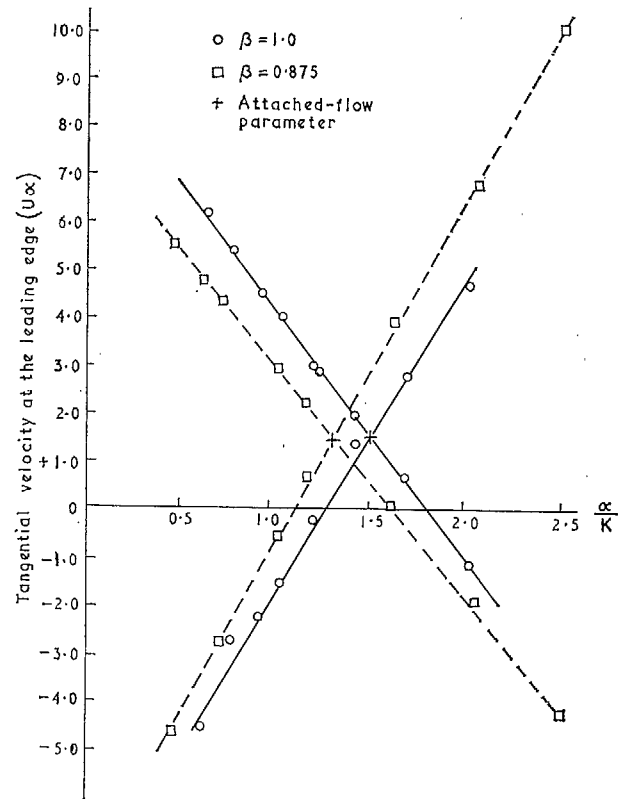


FIG. 8. Attached incidence of parabolic wing.

(89839) Wt. 65/1418 K.S 7/64 HW.

10

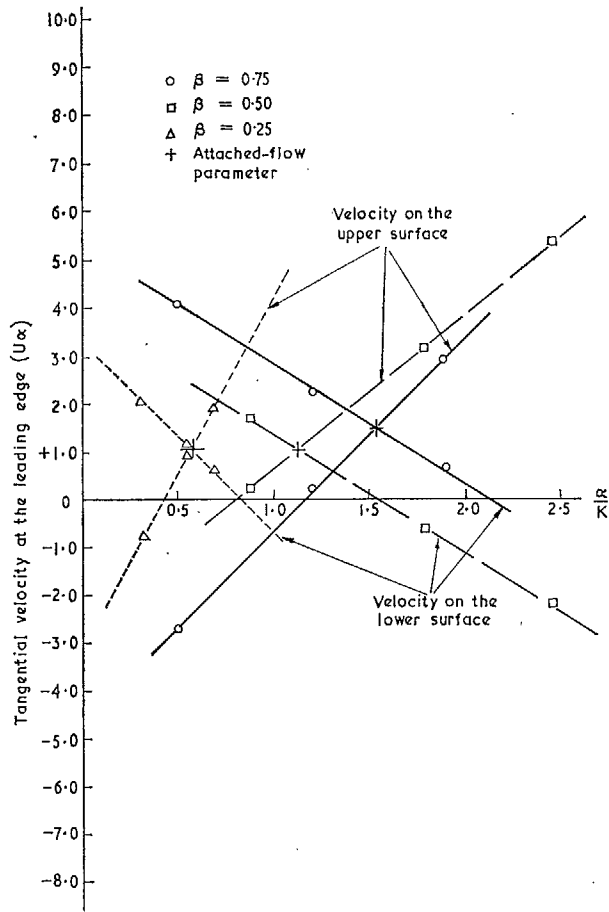


FIG. 9. Elliptical-wing results.

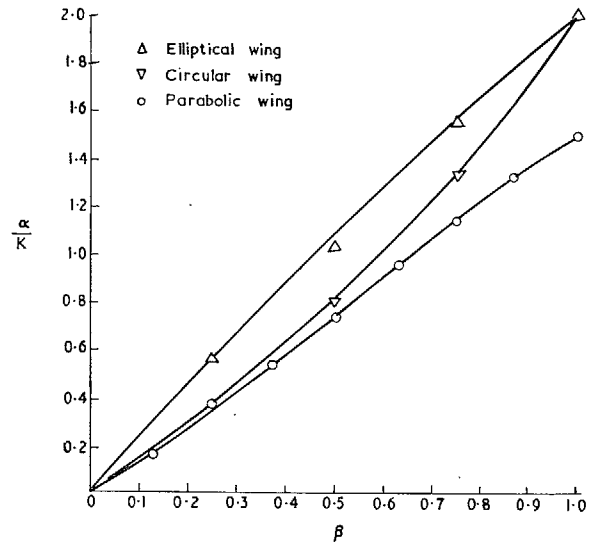


FIG. 10. The attached incidence of various cambered wings.

# Publications of the Aeronautical Research Council

## ANNUAL TECHNICAL REPORTS OF THE AERONAUTICAL RESEARCH COUNCIL (BOUND VOLUMES)

- 1942 Vol. I. Aero and Hydrodynamics, Aerofoils, Airscrews, Engines. 75s. (post 2s. 9d.)  
Vol. II. Noise, Parachutes, Stability and Control, Structures, Vibration, Wind Tunnels. 47s. 6d. (post 2s. 3d.)
- 1943 Vol. I. Aerodynamics, Aerofoils, Airscrews. 80s. (post 2s. 6d.)  
Vol. II. Engines, Flutter, Materials, Parachutes, Performance, Stability and Control, Structures. 90s. (post 2s. 9d.)
- 1944 Vol. I. Aero and Hydrodynamics, Aerofoils, Aircraft, Airscrews, Controls. 84s. (post 3s.)  
Vol. II. Flutter and Vibration, Materials, Miscellaneous, Navigation, Parachutes, Performance, Plates and Panels, Stability, Structures, Test Equipment, Wind Tunnels. 84s. (post 3s.)
- 1945 Vol. I. Aero and Hydrodynamics, Aerofoils. 130s. (post 3s. 6d.)  
Vol. II. Aircraft, Airscrews, Controls. 130s. (post 3s. 6d.)  
Vol. III. Flutter and Vibration, Instruments, Miscellaneous, Parachutes, Plates and Panels, Propulsion. 130s. (post 3s. 3d.)  
Vol. IV. Stability, Structures, Wind Tunnels, Wind Tunnel Technique. 130s. (post 3s. 3d.)
- 1946 Vol. I. Accidents, Aerodynamics, Aerofoils and Hydrofoils. 168s. (post 3s. 9d.)  
Vol. II. Airscrews, Cabin Cooling, Chemical Hazards, Controls, Flames, Flutter, Helicopters, Instruments and Instrumentation, Interference, Jets, Miscellaneous, Parachutes. 168s. (post 3s. 3d.)  
Vol. III. Performance, Propulsion, Seaplanes, Stability, Structures, Wind Tunnels. 168s. (post 3s. 6d.)
- 1947 Vol. I. Aerodynamics, Aerofoils, Aircraft. 168s. (post 3s. 9d.)  
Vol. II. Airscrews and Rotors, Controls, Flutter, Materials, Miscellaneous, Parachutes, Propulsion, Seaplanes, Stability, Structures, Take-off and Landing. 168s. (post 3s. 9d.)
- 1948 Vol. I. Aerodynamics, Aerofoils, Aircraft, Airscrews, Controls, Flutter and Vibration, Helicopters, Instruments, Propulsion, Seaplane, Stability, Structures, Wind Tunnels. 130s. (post 3s. 3d.)  
Vol. II. Aerodynamics, Aerofoils, Aircraft, Airscrews, Controls, Flutter and Vibration, Helicopters, Instruments, Propulsion, Seaplane, Stability, Structures, Wind Tunnels. 110s. (post 3s. 3d.)

### Special Volumes

- Vol. I. Aero and Hydrodynamics, Aerofoils, Controls, Flutter, Kites, Parachutes, Performance, Propulsion, Stability. 126s. (post 3s.)
- Vol. II. Aero and Hydrodynamics, Aerofoils, Airscrews, Controls, Flutter, Materials, Miscellaneous, Parachutes, Propulsion, Stability, Structures. 147s. (post 3s.)
- Vol. III. Aero and Hydrodynamics, Aerofoils, Airscrews, Controls, Flutter, Kites, Miscellaneous, Parachutes, Propulsion, Seaplanes, Stability, Structures, Test Equipment. 189s. (post 3s. 9d.)

### Reviews of the Aeronautical Research Council

1939-48 3s. (post 6d.)

1949-54 5s. (post 5d.)

### Index to all Reports and Memoranda published in the Annual Technical Reports

1909-1947

R. & M. 2600 (out of print)

### Indexes to the Reports and Memoranda of the Aeronautical Research Council

Between Nos. 2351-2449

R. & M. No. 2450 2s. (post 3d.)

Between Nos. 2451-2549

R. & M. No. 2550 2s. 6d. (post 3d.)

Between Nos. 2551-2649

R. & M. No. 2650 2s. 6d. (post 3d.)

Between Nos. 2651-2749

R. & M. No. 2750 2s. 6d. (post 3d.)

Between Nos. 2751-2849

R. & M. No. 2850 2s. 6d. (post 3d.)

Between Nos. 2851-2949

R. & M. No. 2950 3s. (post 3d.)

Between Nos. 2951-3049

R. & M. No. 3050 3s. 6d. (post 3d.)

Between Nos. 3051-3149

R. & M. No. 3150 3s. 6d. (post 3d.)

HER MAJESTY'S STATIONERY OFFICE

from the addresses overleaf

© *Crown copyright* 1964

Printed and published by  
HER MAJESTY'S STATIONERY OFFICE

To be purchased from  
York House, Kingsway, London W.C.2  
423 Oxford Street, London W.1  
13A Castle Street, Edinburgh 2  
109 St. Mary Street, Cardiff  
39 King Street, Manchester 2  
50 Fairfax Street, Bristol 1  
35 Smallbrook, Ringway, Birmingham 5  
80 Chichester Street, Belfast 1  
or through any bookseller

*Printed in England*